Co-published by
Institute of Fluid-Flow Machinery
Polish Academy of Sciences
Committee on Thermodynamics and Combustion
Polish Academy of Sciences

http://www.imp.gda.pl/archives-of-thermodynamics/

Investigations of the specific heat capacity of selected heterogeneous materials

Rafał Gałek[a], Joanna Wilk[a*]

[a]Department of Thermodynamics, Rzeeszów University of Technology, Al.Powstańców Warszawy 12, 35-959 Rzeszów, Poland
*Corresponding author email: joanwilk@prz.edu.pl

Received: 28.12.2023; revised: 19.02.2024; accepted: 18.03.2024

Abstract

This paper presents the results of experimental investigations of the basic thermal property – the specific heat capacity of selected heterogeneous materials – graphene oxide rubber composites. The value of specific heat capacity was measured with a PerkinElmer DSC 8000 differential scanning calorimeter using modulated temperature mode of operation. The heterogeneous material under investigation was the graphene oxide/rubber composite, which is used in the production of roller bearing seals. Two types of rubber have been used as the basic matrix of composites: the hydrogenated acrylonitrile butadiene rubber and the fluoroelastomer. Graphene oxide reduced with sodium hypophosphite was applied as a composite filler. The main goals of the work was to expand the database of thermophysical properties of materials and to investigate the influence of material heterogeneity on the results of specific heat capacity measurements obtained with small-sized test samples.

Keywords: Specific heat capacity; Heterogeneous material; Rubber composite; Modulated temperature; StepScan mode

Vol. 45(2024), No. 2, 91–98; doi: 10.24425/ather.2024.150855

Cite this manuscript as: Gałek, R., & Wilk, J. (2024). Investigations of the specific heat capacity of selected heterogeneous materials. *Archives of Thermodynamics*, 45(2), 91−98.

1. Introduction

Nowadays, materials with a heterogeneous structure are becoming more and more important in technology. One class of such materials encompasses the rubber-based composites filled with nanoparticles in a form of various allotropes of carbon. Both the synthetic and natural rubber are used as a basic matrix in such composite materials. Graphene oxide (GO) may be used as a filling material [1−3], since it improves the mechanical properties and also changes thermal characteristics of the composite. One of the applications of rubber-based composites is the production of the roller bearing seals. The operating temperature of the bearing largely determines the type of the base rubber of composite material. Improving thermal properties of composites with the use of the reduced graphene oxide (rGO) as a filling results in more intensive dissipation of heat generated in the bearing. Thus, the knowledge about physical properties of graphene oxide/rubber composites with heterogeneous structure gains in importance. Thermal conductivity, thermal diffusivity and specific heat capacity are the main important thermophysical properties describing the phenomena of heat transport in materials. For composites with heterogeneous structure it may be difficult to clearly determine these parameters due to the formation of agglomerates and clusters of the filler material.

Nomenclature

A – thermal diffusivity, m^2/s
c_p – specific heat capacity, J/(kg·K)
k – thermal conductivity, W/(m·K)
m – mass, kg
Q – heat, J
$\dot{Q}$ – thermal power, W
t – time, s
T – temperature, °C, K
u – uncertainty
w – weight concentration, %

Greek symbols
δ – correction
ρ – density, kg/m^3
σ – deviation

Abbreviations and Acronyms
DSC − differential scanning calorimetry
FKM − fluoroelastomer
HNBR − hydrogenated acrylonitrile butadiene rubber
HR − heating rate
MT − modulated temperature
rGO − reduced graphene oxide
SEM − scanning electron microscope

Investigations of thermophysical properties of the composites are conducted using both commercial equipment and other unconventional research methods. In some cases the research methods need small samples of investigated materials, thus the heterogeneity can greatly influence test results. Thermal conductivity may be measured directly with the guarded hot plate method [4] or indirectly from the thermal diffusivity measured with a laser flash method [5], either with commercial equipment [6] or unconventional transient techniques [7−9]. The calculation of the value of thermal conductivity uses the basic formula defining the thermal diffusivity in the equation of transient heat conduction. Hence, the thermal conductivity k is equal to the product:

$$k = a \cdot \rho \cdot c_p, \tag{1}$$

where: a – thermal diffusivity, c_p – specific heat capacity, ρ – density.

As can be seen, determination of the thermal conductivity also requires measurements of the specific heat capacity. Heat capacity c_p is one of the basic thermophysical properties of the material. Determining the specific heat capacity is crucial in heat transfer problems, since c_p is an important thermophysical property in predicting heat transfer efficiency. Specific heat capacity is often measured with differential scanning calorimetry method (DSC). In the case of heterogeneous materials like graphene oxide/rubber composites, the use of DSC method causes difficulties in analyzing the measurement results as they may be affected by the small size of the test samples. Therefore, the knowledge about the impact of the material heterogeneity on the investigation results is advisable.

The main goals of the present work are to expand the database of thermophysical properties of the selected graphene oxide/rubber composites with the specific heat capacity values and to investigate the influence of material heterogeneity on the results of DSC measurements. Two different types of rubber: hydrogenated acrylonitrile butadiene rubber and fluoroelastomer were used as the basic matrices of the tested composites. The graphene oxide reduced with sodium hypophosphite acted as a filling material. Specific heat capacity was measured with differential scanning calorimetry method in modulated temperature regime.

2. Materials and methods

2.1. Characteristic of the investigated materials

In the present study the selected graphene oxide/rubber composites, that are used for the production of the roller bearing seals, were investigated experimentally. Two types of rubber were used as the basic matrix of the composites: hydrogenated acrylonitrile butadiene rubber (HNBR) and fluoroelastomer (FKM). Graphene oxide reduced with sodium hypophosphite (rGO) was used as a composite filler. The rGO has an appearance of grey powder, bulk density of $0.019 g/cm^3$ and specific surface area of $266 m^2/g$ [4]. The specific heat capacity and thermal conductivity of GO are approximately 700 J/(kg K) [10] and from several to over two thousands W/(m K) respectively, depending on the form of graphene oxide used [11,12].

The example of the scanning electron microscope (SEM) image of the rGO nanoparticles is presented in Fig. 1.

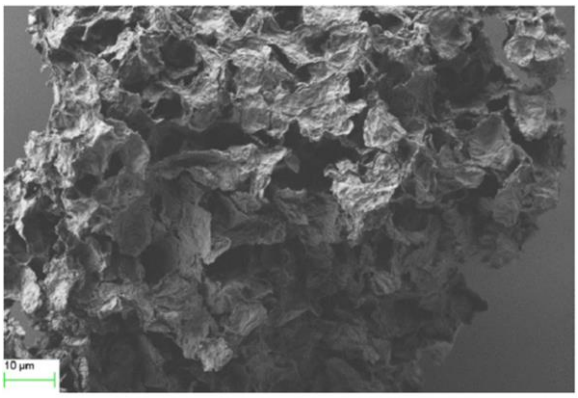

Fig. 1. SEM image (magnification ×1000) of the reduced graphene oxide nanoparticles applied as a filler in tested composites [4].

A conventional method was used to prepare the composite materials: a precisely measured amount of rGO was directly dispersed in the basic rubber matrix during the rolling process [4]. After the process, the weight and the density of rGO/rubber composites were determined using the basic volumetric weighing method. An accuracy of density determination was

±0.003 g/cm^3. The weight concentration of rGO was calculated from the equation:

$$w = \frac{m_{\mathrm{rGO}}}{m_{\mathrm{BM}}+m_{\mathrm{rGO}}}, \tag{2}$$

where m_{BM} is a mass of the composite base matrix.

Figure 2 presents a sample scanning electron microscope (SEM) image of the cross-sectional area of the HNBR composite with a weight concentration of rGO equal to 2.5%.

The basic characteristics of investigated materials including weight concentration of rGO, density and thermal conductivity are presented in Table 1.

Thermal conductivity of the investigated composites was measured with the guarded hot plate method [4]. Thermal diffusivity was obtained using less common methods: thermal regular regime method and the step-heating technique [9].

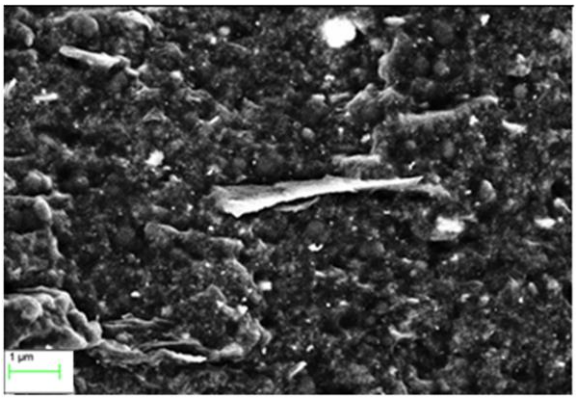

Fig. 2. SEM image (magnification ×10000) of the cross-sectional area of rGO/HNBR composite (H1) [4].

Table 1. Basic properties of investigated composites.

Material	Matrix	Weight concentration of rGO w [%]	Density ρ [kg/m^3]	Thermal conductivity [4] k [W/(m·K)]	Thermal diffusivity a [mm^2/s] (average values [9])
H0	HNBR	0	1 199	0.37	0.160
H1	HNBR	2.5	1 207	0.37	0.162
F1	FKM	1.5	1 885	0.24	0.064
F2	FKM	2.5	1 885	0.25	0.072

2.2. Measuring procedure

Specific heat capacity measurements were carried out using a differential scanning calorimetry (DSC) method, which is a well-established measuring technique in various research areas [13−15]. The main feature of this method is the ability to quickly determine, among others, the specific heat capacity, in a broad temperature range using small amounts of the tested substances. Differential scanning calorimetry involves measuring the change of the difference in the heat flow rate supplied to the sample of the tested material and to a reference sample during the operation of a program that varies the temperature over time. In the classical DSC method the operation mode of the program changing the temperature is characterized by a constant heating rate. It is important that the term "heating rate" is understood in DSC as a rate of temperature change – not to be confused with the heat flow rate (or thermal power), which is in fact a main measured variable in this method. A digital scanning calorimeter may also be operated in variable heating rate regime – techniques utilizing such a mode are collectively known as modulated temperature (MT) methods. In the case of variable heating rate a special modulation term is added to the usual linear change of temperature with time. Modulated-temperature DSC technique may also be applied for the measurements of the specific heat capacity c_p. [13,16,17]. There are several variants of this method [18], one of them being the StepScan mode – a proprietary technique of PerkinElmer - characterized by the temperature vs time function in the form presented in Fig. 3.

In the present study a DSC 8000 calorimeter from PerkinElmer was used for the measurements of specific heat capacity in the StepScan mode. The method involves repeatedly heating

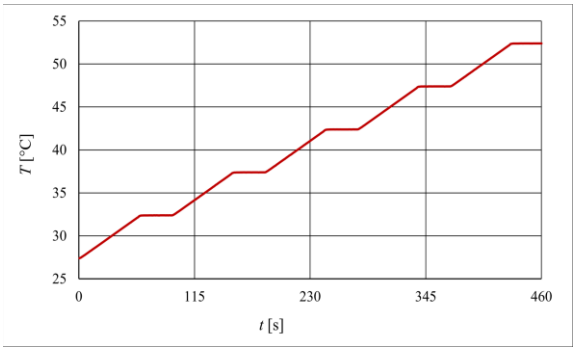

Fig. 3. Variation of the temperature with time in the StepScan mode.

the sample and then maintaining it in isothermal conditions for several dozen seconds. During heating periods, the value of the supplied thermal power depends on the specific heat of the material and on possible phase changes, while in isothermal periods - only on kinetic phenomena. As a variant of temperature-modulated differential scanning calorimetry, the StepScan method is typically used in situations where phase transitions or chemical reactions are expected within the temperature range being investigated. In the present study, the use of the StepScan mode was motivated by the fact that in this method the value of the integral of the recorded relationship between thermal power $\dot{Q}$ and the time t is used to determine the c_p [18] instead of the instantaneous values of $\dot{Q}$ utilized in classic DSC experiment. Hence:

$$c_p = \frac{Q}{m\Delta T}, \tag{3}$$

where: Q – heat supplied to the test sample during the single heating period (integral of $\dot{Q}(t)$), m – sample mass, ΔT – temperature increase during the single heating period.

Calculation of the specific heat capacity from the integral of $\dot{Q}(t)$ for small temperature changes in a short time makes this method practically insensitive to one of the most significant problems of differential scanning calorimetry – the drift of the calorimeter baseline. The baseline is the reaction of the DSC system with both crucibles empty for the prescribed heating rate program in the classical DSC. In standard DSC method of specific heat capacity measurement, where c_p is determined from the value of the thermal power $\dot{Q}$ supplied to the material sample at a given moment and at a specific temperature, the drift of the baseline may significantly affect the measurement results, especially when a single experiment covers a wide temperature range, i.e. it lasts longer. In the StepScan method, the influence of the drift practically does not occur, because the value used in the calculation is the area under the curve $\dot{Q}(t)$ based at the level of neighbouring isotherms. Since the temperature change in a single heating period is small, the isotherms bounding that period are so close in time that significant baseline drift could not have appeared between them. Thus, due to the very short times required for each measuring step, the specific heat capacity value obtained with the StepScan method is not sensitive to baseline drifts, even at higher temperatures.

In the present work the parameters of the StepScan method included a heating rate (HR) of 5 K/min and a temperature increase of 5 K for each heating period. The temperature interval ΔT was selected in such a way that the values of the thermal energy Q for the tested samples were close to the values observed during the caloric calibration of the apparatus using sapphire samples. Such a choice aimed to keep the actual measurement conditions close to the conditions of the calibration, which, in theory, should positively affect the accuracy of measurement of Q. The selection of the heating rate value was based on the rationale derived from the form of the $\dot{Q}(t)$ relationship recorded on the graph. The heating rate was selected low enough so that the $\dot{Q}(t)$ dependence within one step was not dominated by transient state, i.e. so that after the increase of $\dot{Q}$ there was relative stabilization period of at least about 30s. At the same time the HR value was chosen to be high enough so that the maximum of each step was above the value of $\dot{Q}$ = 1 mW, since at lower values it would be expected that the relative accuracy of the calorimeter signal measurement would be decreased.

Sample graphs of the thermal power supplied to the tested sample as a function of temperature and time in StepScan method are shown in Fig. 4. The data presented in the graphs in Fig. 4. are consistent with the temperature vs time dependence from Fig. 3.

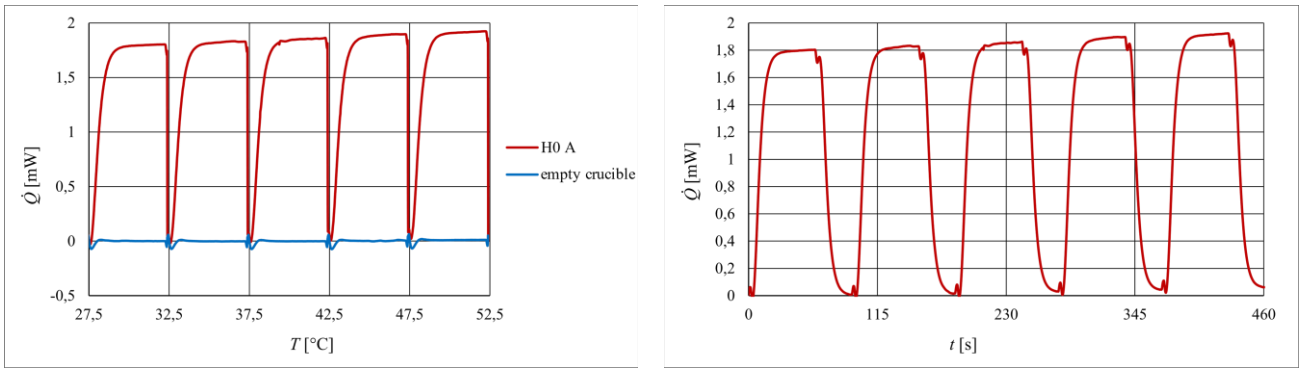

Fig. 4. Thermal power supplied to the test sample in the StepScan mode vs. temperature and time.

2.3. Uncertainty analysis

The uncertainty of the specific heat capacity measurement with StepScan differential scanning calorimetry is affected by the uncertainties of the measurements of temperature, thermal energy and the sample mass. Before the measurements, the temperature calibration and the caloric calibration had been performed for the apparatus used in present work. The melting points of indium and zinc had been used as a temperature standards for the calibration of the temperature measuring subsystem. The thermal power measurement subsystem of the calorimeter had been calibrated using the specific heat capacity of the sapphire standard sample. The mass of the investigated samples was in the range of 13–19 mg. The samples were weighed with a RADWAG XA 210/Y analytical balance with a resolution of 0.01 mg.

The uncertainty of the temperature measurement depends on the uncertainty of the temperature calibration, uncertainty of the certified melting point of the material used in temperature calibration, uncertainty of the thermal lag measurement and the uncertainty caused by linear interpolation of the temperature sensor characteristic [19].

In the StepScan method the temperature measurement takes place in isothermal conditions, before and after each heating step. Therefore, the dynamic correction accounting for thermal lag does not apply here and there is no need to take its uncertainty into account. The manufacturer of the DSC system provides the information that the temperature sensor embedded into calorimeter is a platinum resistance thermometer, however data about the polynomial used in the software for the interpolation of its characteristic are not disclosed. Therefore, the only possible assumption is that general good practices and international standards have been observed regarding application of the temperature sensor. Since both IEC 60751 and ASTM E1137 rec-

ommend using at least second order polynomial for the interpolation of the characteristic of resistance thermometers, the correction due to the linear interpolation is not applicable and its uncertainty is not taken into account. Thus, the standard uncertainty of the temperature measurement takes a form:

$$u(T) = \sqrt{u^2(\delta T_{\text{calib}}) + u^2(\delta T_{\text{mat}})}, \quad (4)$$

where: $u(\delta T_{\text{calib}})$ – uncertainty of the temperature calibration; $u(\delta T_{\text{mat}})$ – uncertainty of the certified melting point of the material used for calibration.

According to [18], the standard uncertainty of the calibration correction $u(\delta T_{\text{calib}})$ may be determined by repeated measurements of the melting temperature of the calibration standard material, i.e. as the standard uncertainty type A [20]. In turn, the uncertainty $u(\delta T_{\text{mat}})$ should be based on the uncertainty of the phase transition temperature of the material used for calibration. In the StepScan method, the c_p value is determined from Eq. (3), where the energy Q is the integral of thermal power $\dot{Q}$ with respect to time. It can be assumed that the main sources of measurement uncertainty of thermal energy Q are analogous to the sources of measurement uncertainty of thermal power $\dot{Q}$. The standard uncertainty of the thermal energy supplied to the tested sample during the measurement may be written as:

$$u(Q) = \sqrt{u^2(Q_s) + u^2(\delta Q_{\text{cal}}) + u^2(\delta Q_{\text{mat}})}, \quad (5)$$

where: $u(Q_s)$ – uncertainty of the determination of thermal energy supplied to the sample during actual measurement (type A), $u(\delta Q_{\text{cal}})$ – uncertainty of the calibration correction, $u(\delta Q_{\text{mat}})$ – uncertainty of the correction resulting from the uncertainty of the calibration material specific heat capacity value.

Uncertainties $u(Q_s)$ and $u(\delta Q_{\text{cal}})$ may be obtained by repeated measurements of the heat supplied to the test sample and the calibration sample, respectively. The value of $u(\delta Q_{\text{mat}})$ is determined as a combined uncertainty of zero-valued correction δQ_{mat} reflecting the conditions during caloric calibration procedure. It is assumed that the certified specific heat capacity value of the calibration material is exact, i.e. $\delta c_p = 0$ and the standard uncertainty of this assumption simplifies to:

$$u(\delta Q_{\text{mat}}) = \sqrt{\left(u(\delta c_{p,\text{cal}}) m_{\text{cal}} \Delta T_{\text{cal}}\right)^2} = \left|u(\delta c_{p,\text{cal}}) m_{\text{cal}} \Delta T_{\text{cal}}\right|, \quad (6)$$

where m_{cal} and ΔT_{cal} are the mass of the calibration sample and the temperature interval of the single heating period during calibration, respectively; $u(\delta c_{p,\text{cal}})$ is the standard uncertainty of the $c_{p,\text{cal}}$ value.

According to [21], the uncertainty of the mass measurement with an analytical balance depends on the repeatability, reproducibility, non-linearity, the standard uncertainty of the calibration and the difference between calibration temperature and measurement temperature. The latter component is neglected in present work, since the temperature in the lab was precisely maintained at the same value during calibration and the actual measurements. The uncertainty of the mass measurement may, therefore, be expressed as [16]:

$$u(m) = \sqrt{S_{\text{r}}^2 + S_{\text{env}}^2 + \frac{a_{\text{L}}^2}{3} + u^2{}_{\text{cal}}}, \quad (7)$$

where: S_{r} and S_{env} are the repeatability and reproducibility, respectively, determined on the basis of the statistical analysis; a_{L} – maximum deviation due to non-linearity as stated by the balance manufacturer; u_{cal} – calibration uncertainty depending on the standard uncertainty of the mass reading and the mass standard used for calibration.

The standard uncertainty of the specific heat capacity measurement with the StepScan mode of MT-DSC method is given by the formula:

$$u(c_p) = \sqrt{\left(\frac{\partial c_p}{\partial Q} u(Q)\right)^2 + \left(\frac{\partial c_p}{\partial m} u(m)\right)^2 + 2\left(\frac{\partial c_p}{\partial T} u(T)\right)^2}, \quad (8)$$

where the partial derivatives (sensitivity coefficients): $\frac{\partial c_p}{\partial Q}$, $\frac{\partial c_p}{\partial m}$, $\frac{\partial c_p}{\partial T}$ are determined on the basis of Eq. (3).

3. Results and discussion

Measurements were performed for five distinct samples of each investigated material with an exception of expectedly the most homogeneous one – H0, for which only 3 samples were tested. The samples were extracted from different locations of a larger piece of composite material. As a final result of the investigation the values of specific heat capacity in the temperature range 10−110°C were obtained. Results of the measurements for materials H0, H1 and F1, F2 are presented in Fig. 5 and Fig 6. The chart in Fig.5 includes the values of c_p for three samples of the base matrix material HNBR (H0) and for five samples of the rGO/HNBR (H1) composite with the weight concentration of rGO equal to 2.5%. In turn, Fig.6 presents the results of five measurements for the rGO/FKM composite also characterized by weight concentration of w = 2.5% (F2) and w = 1.5% (F1). It may be seen, that the dispersion of the c_p values for different samples of a given material is very low.

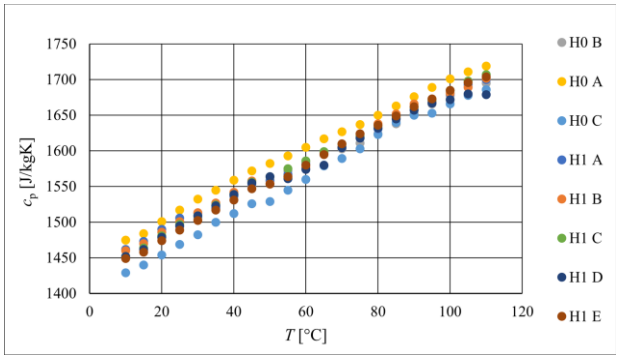

Fig. 5. Specific heat capacity of composites based on HNBR matrix. A, B, C, D, E – results for different samples of the tested material.

As follows from the Eq. (3), the StepScan method basically determines the average value of specific heat capacity in a single heating period, therefore, for ΔT = 5 K, the presented values of c_p for a given temperature should in fact be understood as aver-

age values within the range of ±2.5 K in relation to that temperature.

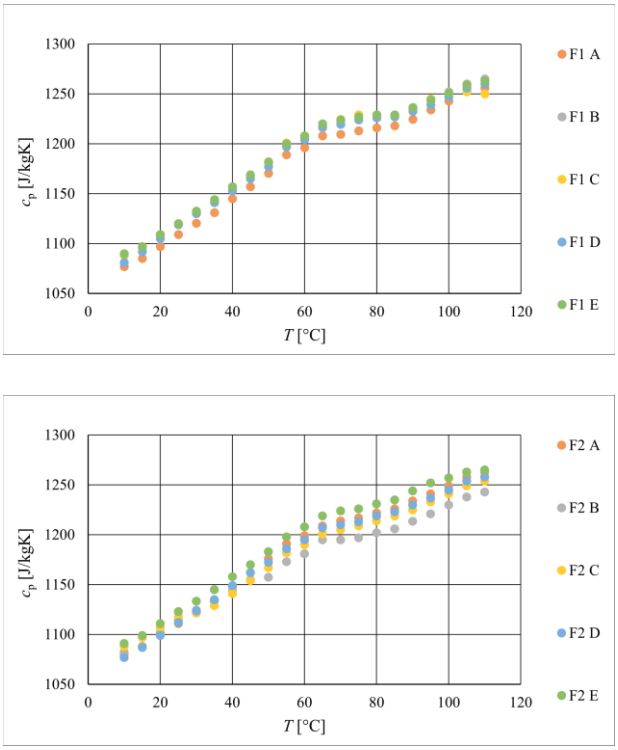

Fig. 6. Specific heat capacity of composites based on FKM matrix. A, B, C, D, E – results for different samples of the tested material.

Based on the analysis presented in Section 2.3, the standard uncertainties of each measurand affecting the uncertainty of c_p measurement were determined. An example of the uncertainty budget for the H0 material at 40°C is presented in Table 2.

Table 2. Uncertainty budget of the specific heat measurement of H0 material at 40°C.

Quantity X_i	Standard uncertainty $u(X_i)$	Sensitivity coefficient $\frac{\partial c_p}{\partial X_i}$
Q	$1.08 \cdot 10^{-3}$ [J]	14.25 [1/(g K)]
m	$6.01 \cdot 10^{-5}$ [g]	-108.5 [J/(g^2 K)]
T	0.1 [K]	0.3 [J/(g K^2)]
c_p	0.046 [J/(g K)]	–––––

The standard uncertainty of the c_p value for the sample estimation presented in Table 2 is $u(c_p)$ = 0.046 J/(g K), which corresponds to relative standard uncertainty of 3%. Assuming the coverage factor of 2 resulting in the level of confidence of approximately 95%, the expanded uncertainty of c_p measurement is 0.092 J/(g K) and the relative expanded uncertainty is 6%.

As a measure of dispersion of the results for a single material, the relative standard deviation σ_{rel} was calculated according to the formula:

$$\sigma_{rel} = \frac{1}{c_{p,m}} \sqrt{\frac{1}{5} \sum_{i=1}^{5} \left(c_{p,i} - c_{p,m}\right)^2}, \qquad (9)$$

where: $c_{p,m}$ - the average value of specific heat capacity calculated from all samples of given material, $c_{p,i}$ - specific heat capacity of the i-th sample.

Sample results of the average specific heat capacity and relative standard deviation obtained for the material F2 at five temperatures are presented in Table 3.

Table 3. Specific heat for rGO/FKM composite with w=2.5% (F2).

T [°C]	$c_{p,m}$ [J/(kgK)]	σ_{rel} [%]
10	1083.6	0.48
25	1115.6	0.40
60	1194.6	0.75
90	1229.3	0.82
110	1256.6	0.62

The calculated relative standard deviation for rGO/FKM composite F2 is below 1% over the entire temperature range considered. Similar results were observed for samples taken from other composites.

Since the dispersion of the results is well below the measurement uncertainty, it may be concluded that for the investigated materials the heterogeneity of the composite does not affect the c_p value in the extent that may be detected with applied experimental method.

The average values of the specific heat capacity for H0, H1, F1 and F2 are presented in Fig. 7 as a function of temperature.

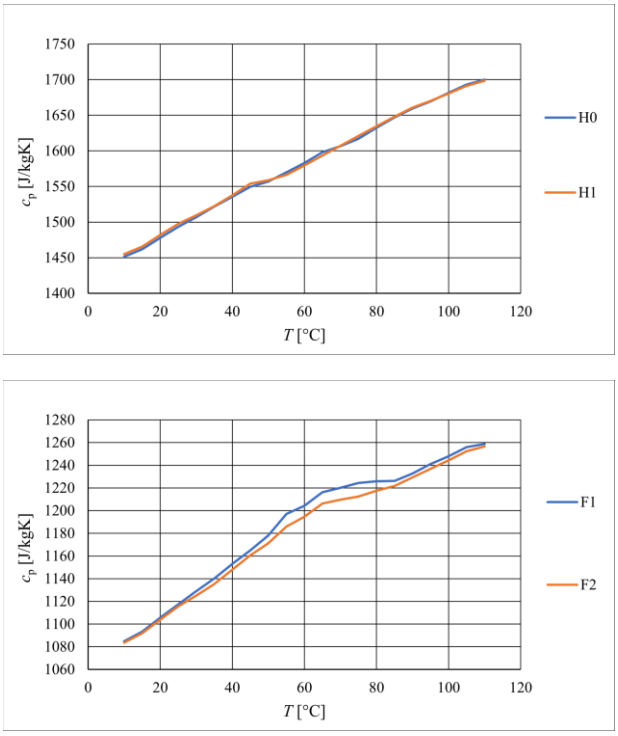

Fig. 7. Specific heat capacity vs. temperature for HNBR and FKM-based GO/rubber composites.

As may be seen, in the case of H0 and H1 materials, the values of specific heat capacity basically coincide in whole temperature range. For FKM-based composites there is a slight deviation in c_p value between F1 and F2 materials in the temperature range 50−80°C, however the value of the observed difference is much lower than the measurement uncertainty, therefore it cannot be considered an evidence of actual disparity between these materials in terms of c_p value. Nonetheless, decreasing specific heat value with increasing rGO content would be explainable [17], since the specific heat capacity of graphene oxide (approximately 700 J/(kg K) [10]) is lower than c_p of fluoroelastomer.

4. Conclusions

In the present study the results of the specific heat capacity measurements performed for reduced graphene oxide/rubber composites are reported. The FKM and HNBR rubbers were used as matrices of tested materials while graphene oxide reduced with sodium hypophosphite was used as a filler material. Specific heat capacity was measured with StepScan method being a variant of the modulated temperature differential scanning calorimetry. Due to the heterogeneity of the composites tested, several samples of each material were investigated. The study includes an estimation of the measurement uncertainty of the applied method.

The following conclusions may be formulated on the basis of performed investigation and the obtained results:

- the StepScan mode of DSC method enabled the measurement of the specific heat capacity of rGO/rubber composites with reasonable accuracy;
- a clear increase in c_p of tested materials with temperature was found;
- due to the heterogeneity of the investigated composites and small size of the test samples, the differences in c_p results obtained from distinct material samples were expected, however, the observed differences turned out to lay well within the measurement uncertainty.

References

[1] Wen, Y., Yin, Q., Jia, H., Yin, B., Zhang X., Liu, P., Wang, J., Ji Q., & Xu, Z. (2017). Tailoring rubber-filler interaction and multifunctional rubber nanocomposites by usage of graphene oxide different oxidation degrees. *Composites Part B: Engineering*, 124, 250−259. doi: 10.1016/j.compositesb.2017.05.006

[2] Lim, L.P., Juan, J.C., Huang, N.M., Goh, L.K., Leng, F.P., & Loh, Y.Y. (2019). Enhanced tensile strength and thermal conductivity of natural rubber graphene composite properties via rubber-graphene interaction. *Materials Science and Engineering B*, 246, 112−119. doi: 10.1016/j.mseb.2019.06.004

[3] Zheng, L., Jerrams, S., Xu, Z., Zhang, L., , L., & Wen, S. (2020). Enhanced gas barrier properties of graphene oxide/rubber composites with strong interfaces constructed by graphene oxide and sulfur. *Chemical Engineering Journal*, 383, 123100. doi: 10.1016/j.cej.2019.123100

[4] Wilk, J., Smusz, R., Filip, R., Chmie,l G., & Bednarczyk, T. (2020). Experimental investigations on graphene oxide/rubber composite thermal conductivity. *Scientific Reports*, 10, 15533. doi: 10.1038/s41598-020-72633-z

[5] Parker, W.J., Jenkins, R.J., Butler, C.P., & Abbott, G.L. (1961). Flash Method of Determining Thermal Diffusivity, Heat Capacity, and Thermal Conductivity. *Journal of Applied Physics*, 32(9), 1679−1684. doi: 10.1063/1.1728417

[6] Bocchini, G.F., Bovesecchi, G., Coppa, P., Corasaniti, S., Montanari, R., & Varone, A. (2016). Thermal Diffusivity of Sintered Steels with Flash Method at Ambient Temperature. *International Journal of Thermophysics*, 37(4), 1−14. doi: 10.1007/s10765-016-2050-4

[7] Kruczek, T., Adamczyk, W.P., & Białecki, R.A. (2013). In Situ Measurement of Thermal Diffusivity in Anisotropic Media. *International Journal of Thermophysics*, 34, 467−485. doi: 10.1007/s10765-013-1413-3

[8] Adamczyk, W., Białecki, R., Orlande, H.R.B., & Ostrowski, Z. (2020). Nondestructive, real time technique for in-plane heat diffusivity measurements. *International Journal of Heat and Mass Transfer*, 154(3), 119659. doi: 10.1016/j.ijheatmasstransfer.2020.119659

[9] Wilk, J., Smusz, R., & Filip, R. (2023). Experimental investigations on thermal diffusivity of heterogeneous materials. *Experimental Thermal and Fluid Science*, 144(9), 110868. doi: 10.1016/j.expthermflusci.2023.110868

[10] Al-Douri, Y. (2022). *Graphene, Nanotubes and Quantum Dots-Based Nanotechnology. Fundamentals and Applications*. (1st Edn.). Woodhead Publishing, Elsevier, Kidlington.

[11] Mahanta, N.K., & Abramson, A.R. (2012). Thermal conductivity of graphene and graphene oxide nanoplatelets. *13th IEEE ITHERM Conference*, 30 May – 01 June, San Diego, USA. doi: 10.1109/ITHERM.2012.6231405

[12] Meng ,Q. L., Liu, H., Huang, Z., Kong, S., Jiang, P., & Bao, X. (2018). Tailoring thermal conductivity of bulk graphene oxide by tuning the oxidation degree. *Chinese Chemical Letters*, 29(5), 711−715. doi: 10.1016/J.CCLET.2017.10.028

[13] McHugh, J., Fideu, P., Herrmann, A., & Stark, W. (2010). Determination and review of specific heat capacity measurements during isothermal cure of an epoxy using TM-DSC and standard DSC techniques. *Polymer Testing*, 29(6), 759–765. doi: 10.1016/j.polymertesting.2010.04.004

[14] Bernardes, C.E.S., Joseph, A., & Minas da Piedade, M.E. (2020). Some practical aspects of heat capacity determination by differential scanning calorimetry. *Thermochimica Acta*, 687, 178574. doi: 10.1016/j.tca.2020.178574

[15] Jiao, Y., Liu, C.F., Cui, X.P., Zhang, J., Huang, L.J., & Geng, L. (2022). A new approach for measurement of the low-temperature specific heat capacity. *Measurement*, 203, 111892. doi: 10.1016/j.measurement.2022.111892

[16] Gill, P.S., Sauerbrunn, S.R., & Reading, M. (2014). Modulated differential scanning calormetry, *Journal of Thermal Analysis*, 40, 931−939. doi: 10.1007/BF02546852

[17] Riviere, L., Causse, N., Lonjon, A., Dantras, E., & Lacabanne, C. (2016). Specific heat capacity and thermal conductivity of PEEK/Ag nanoparticles composites determined by Modulated-Temperature Differential Scanning Calorymetry. *Polymer Degradation and Stability*, 127, 98−104. doi: 10.1016/j.polymdegradstab.2015.11.015.

[18] Höhne, G.W.H., Hemminger, W.F., & Flammersheim, H.J. (2003). *Differential Scanning Calorimetry* (2nd Edn.), Springer-Verlag, Berlin Heidelberg.

[19] Rudtsch, S. (2002). Uncertainty of heat capacity measurements with differential scanning calorimeters. *Thermochimica Acta*, 382 (1−2), 17–25. doi: 10.1016/S0040-6031(01)00730-4

[20] BIPM, IEC, IFCC, ILAC, ISO, IUPAC, IUPAP, OIML (2008). *Evaluation of measurement data - Guide to the expression of uncertainty in measurement* (1st Edn.) Joint Committee for Guides in Metrology, JCGM 100.

[21] González, A.G., & Herrador, M.Á. (2007). The assessment of electronic balances for accuracy of mass measurements in the analytical laboratory. *Accreditation and Quality Assurance*, 12(1), 21−29. doi: 10.1007/s00769-006-0214-9